Journal of Material Sciences & Engineering

Research Article **Open Access**

Effect of Two-Step Ion Implantation and Microwave Annealing on Dopants Activation in Silicon-Germanium

Tai-Chen Kuo*, Chao-Yi Lin and Wen-Hsi Lee

Department of Electrical Engineering, National Cheng Kung University No.1, University Road, Tainan City 701, Taiwan

Abstract

The strain engineering of the source/drain has been applied from the N45 till now. When the size of the transistor is reduced continuously, it is necessary to increase the germanium concentration to add more stress, but it reduces boron concentration with increasing the germanium. The use of ion implantation compensates for the boron concentration well, while caused some problems, including ion implantation damage, diffusion, and activation of dopant ions. Therefore, to activate dopants by tuning different Ge content or pre-amorphized implantation. In the meantime, in order to cope with the low-temperature process for Ge, microwave annealing was added to compare with rapid thermal annealing.

In this paper, silicon germanium film covered with Si, Ge and uncovered before ion implantation is investigated. The sample deposit with Ge capping layer undergoes surface loss after annealing, and the Si capping layer can effectively prevent the surface from roughness. Next, the trend of the Boron activation in SiGe alloys with different Ge contents is discussed. The boron activation level increases with the increase of Ge content, but the trend will gradually saturate, and even segregate to cause the device degradation. From 20% to 40% Ge with a dose of B (ISD 3.2×10^{20} cm^{-2}+I/I 3×10^{15} cm^{-2} and 2×10^{15} cm^{-2}), Si0.65Ge0.35 is an optimum value. For dopants activation in SiGe material, the thermal process is dominant, but the influence of SiGe composition is gradually increasing. The control of in-situ doping concentration has become an important issue. Finally, the diffusion and electrical properties of various species pre-amorphized implantation, repair implant damage by microwave annealing and rapid thermal annealing are investigated. Boron distribution, sheet resistance, and mobility were checked to infer the activation level and defect evolution. The best performance is the sample with Ge PAI, and it can effectively enhance the boron activation by microwave annealing while preventing the diffusion.

Keywords: Silicon-Germanium material; Microwave annealing; Dopants activation; Hole mobility

Introduction

In scaling down the physical gate length of metal-oxide-semiconductor field effect transistors (MOSFETS) to 10/7 nm by 2017 to meet the roadmap of IMEC in 2015 [1], several challenges must be overcome. One of the main challenges is Si-based transistors have reached many dimensional and material limitations, so it is more urgent to study new materials to replace silicon. According to IMEC logic roadmap, Silicon-Germanium compound has been chosen to be the new promising materials and could replace silicon as channel materials in the future. Like Ge and III–V compound, SiGe has higher hole mobility due to its stress effect. Second, in order to reduce the sheet resistance, it is necessary to increase the active carrier concentration, but at the same time the ultra-shallow junction should be maintained, and the placement of the active doping region cannot be increased by the subsequent annealing. To keep the junction and resistance low, high temperature and short-timed anneals have been widely studied to electrically activate implanted dopants and repair lattice damage created after ion implantation to reduce junction leakage currents. Although these high-temperature annealing methods have demonstrated some successful applications to the source/drain anneal, they all still have a number of problems that make processing more complicated.

MWA is an alternative annealing method operating at low annealing temperatures and longer annealing times than conventional thermal processes. Because heat by microwave is generated within the volume of material, microwaves can effectively activate the dopant at low temperatures without dopant diffusion [2-5]. The MWA technique has also been used for low-temperature fabrication of Ge-based MOSFETs [6] and recrystallization of amorphous Si films [7]. This rapid and uniform heating at relatively low temperatures results in less dopant diffusion [8].

Thompson et al. [8] show evidence that boron-implanted Si can be heated by microwave irradiation without the use of a susceptor. Kohli et al. [9] reported on the effects of high-temperature microwave processing and boron activation in B/BF2 implanted Si. And more studies have shown that dopant in Ge:P [10-13], Si:B [14] and III-V semiconductors [15] can be highly activated by microwave annealing. However, high doses and low energy of B implants in SiGe alloys activated by MWA have not been studied.

In this paper, two-step low-energy ion implantation and low-temperature microwave annealing (MWA) were used to recover and activate boron-implanted SiGe wafers. At the same time, the use of Ge-enhanced B-activated pre-amorphous implants (PAI) has been demonstrated [16,17]. Therefore, in order to study the role of the PAI process in SiGe, pre-amorphized implantation with Si or Ge was studied, followed by two-step low energy B implantation and MWA activation.

*Corresponding author: Tai-Chen Kuo, Department of Electrical Engineering, National Cheng Kung University No.1, University Road, Taiwan City 701, Taiwan, Tel: 886-6-2757575, Extn. 62301; E-mail: mrkuo1116@hotmail.com

Experimental Procedures

The experimental part of this paper consists of three sections:

(a) Different capping layer including Si and Ge were deposited on blanket 12-inch p-type (100) substrates with 30 nm Si0.7Ge0.3 layer. 4 nm Ge capping layer was deposited using an e-beam evaporator technique with a background pressure of 1×10^{-6} Torr. In addition, 4nm Si capping layer was deposited using cluster RF Sputter.

Pre-amorphous implantation process with silicon was used, followed by a boron implant at room temperature. To protect dopant loss during the rapid thermal annealing process, SiO_2 was deposit as a top capping layer. After annealing, the SiO_2 capping layer was removed by HCl.
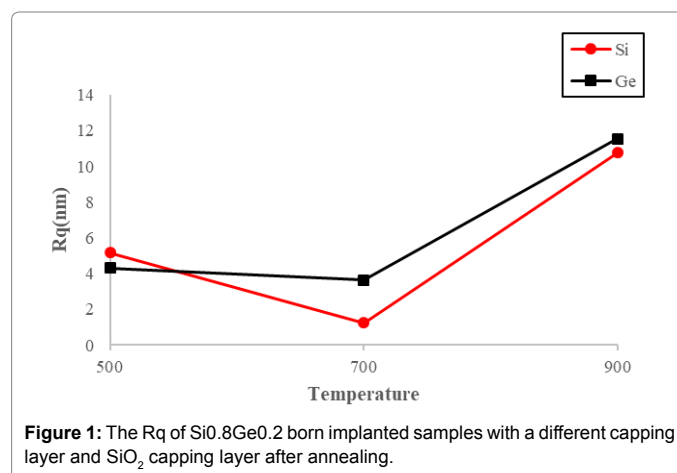
(b) Boron activation in SiGe with different Ge content using RTA and MWA. Si1-xGex epi-layers with different Ge contents (x=0.2, 0.3, 0.35 and 0.4) were deposited by ultra-high vacuum chemical vapor deposition on 12-inch p-type (100) substrates. Boron ions were then implanted in two-steps: first with 2 keV at 3×10^{15} cm^{-2} and second with 1 keV at 2×10^{15} cm^{-2}. A 50 nm SiO_2 capping layer was then deposited. Then, RTA was performed in an N2 atmosphere from 500°C-900°C for 10 s. In order to compare the results to RTA, MWA was also performed with varying power levels: 1P-5P (where 1P is 600 W) for 100 s. After fabrication, the four-point probe and micro-Hall measurements were used to characterize B activation.

(c) Boron activation in SiGe pre-amorphized with Si or Ge implantation using RTA and MWA. A pre-amorphization implant using Si (5.5 keV at 1×10^{15} cm^{-2}) or Ge (10 keV at 1×10^{15} cm^{-2}) ions was performed. Then B was implanted in two steps (first with 2 keV at 3×10^{15} cm^{-2} and second with 1 keV at 2×10^{15} cm^{-2}). Boron-implanted Si0.7Ge0.3 (without PAI) served as a control. Wafers with these three implantation conditions (B, Ge PAI+B, Si PAI+B) were activated by RTA or MWA.

Results and Discussion

To compare the conditions of different capping layers, two different materials (Si and Ge) were deposited and counterparts by an uncovered sample. Then roughness and surface topography of different capping layer materials annealed between 500°C and 900°C by RTA are shown in Figure 1 and Table 1. After RTA annealing, the trend of Rq is all the same, which drop at 700°C then rise at 900°C. At high temperatures, the Rq of Ge capping layer is higher than Si and uncover. In addition, in this temperature range, having a Si capping layer is the most stable.

Next, the sheet resistance has been measured. Table 2 shows the sheet resistance of the Si and Ge capping layer after RTA annealing. The minimum sheet resistance is the Si capping layer annealed at 700°C. But, it starts to increase at 800°C and drop again after 900°C. According to previous research, it reaches the highest activation level at 700°C, but over-temperature annealing about at 800°C caused it to deactivate so the sheet resistance increased. When the annealing temperature comes
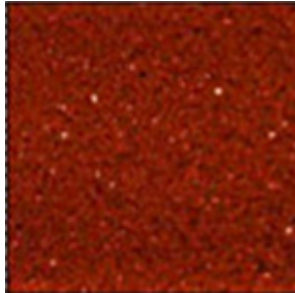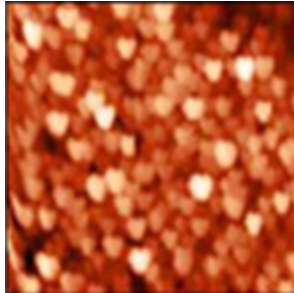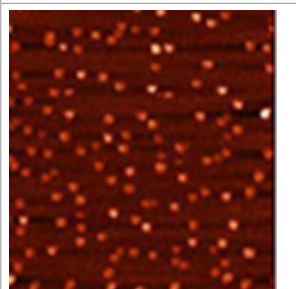

Figure 1: The Rq of Si0.8Ge0.2 born implanted samples with a different capping layer and SiO_2 capping layer after annealing.
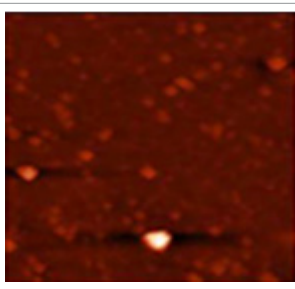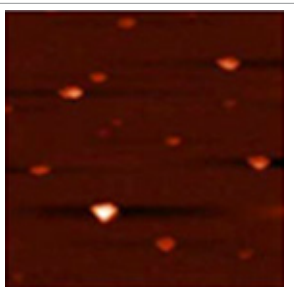
Material/Temperature	500°C	700°C	900°C
Silicon	Rq=5.18 nm	Rq=1.25 nm	Rq=10.76 nm
Germanium	Rq=4.31 nm	Rq=3.63 nm	Rq=11.54 nm

Table 1: The topography of different capping layer annealed between 500°C to 900°C by RTA.

Material/Temperature	500°C	600°C	700°C	800°C	900°C
Silicon	325	268	208	293	249
Germanium	470	323	240	257	377

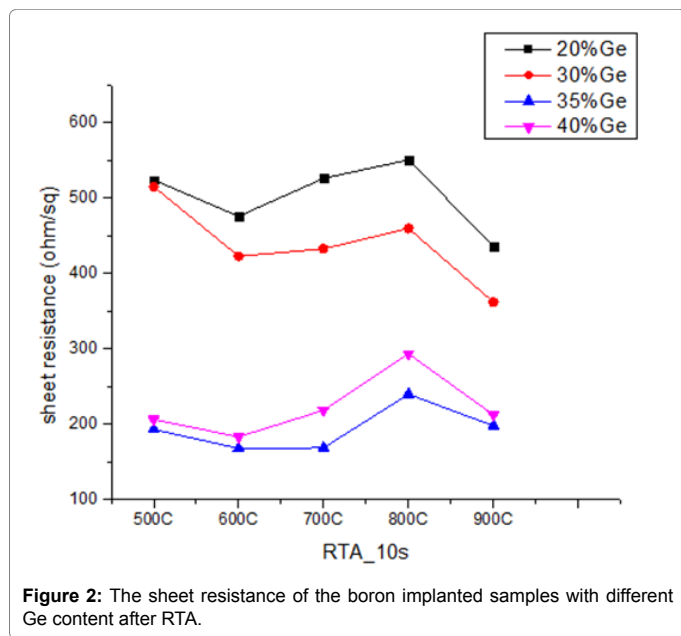**Table 2:** The sheet resistance (ohm/sq.) of different capping layer annealed between 500°C to 900°C by RTA.

Figure 2: The sheet resistance of the boron implanted samples with different Ge content after RTA.

Figure 3: Hall mobility of boron implanted samples with different Ge content after RTA.

to 900°C, the sheet resistance drops again because of the out-diffusion. To sum up the results by surface roughness, topography and sheet resistance, the trend of Ge capping layer and uncovered is identical in the previous experiment. Therefore, it can infer that the Ge capping layer on SiGe may suffer surface loss to cause its behavior similar to uncovered. Conversely, the Si capping layer can effectively prevent the surface from roughness, which in turn reduces its sheet resistance.

Figure 2 shows the sheet resistance of boron implanted samples after RTA annealing at 500°C-900°C. The minimum sheet resistance of 35% Ge contents occurs at 600°C. Also, SiGe with high Ge content has lower sheet resistance than the lower Ge content of SiGe for each temperature. However, over 40% of Ge content will induce a stress effect, because of the strain associated with more Ge atoms occupying the lattice.

The Hall mobility of SiGe with varying Ge content implanted with boron is illustrated in Figure 3. The mobilities range from 20 to 150 $cm^2V^{-1}s^{-1}$. At higher RTA temperatures, the mobility drops dramatically, which may be due to the diffusion and stress relaxation during high-temperature annealing. For SiGe alloys, the mobility increases with increasing Ge content up to 35% Ge content, before decreasing again for 40% Ge content. The results parallel the results for sheet resistance.

To compare with RTA results, MWA annealing was performed with power ranging from 1P to 5P for 100 s. The results for sheet resistant and Hall mobility for different Ge content annealed by MWA are shown in Figures 4 and 5, respectively. The lowest sheet resistance and highest mobility are in 35% Ge content at 3P. Table 3 lists the sheet resistance and mobility of different Ge content annealed by RTA at 600°C and MWA at 3P. It can be observed that the sheet resistance and mobility of SiGe following MWA is better than after RTA. Previous studies of dopant activation in Silicon, Germanium and III-V Group semiconductors have shown that dopants can be fully activated by
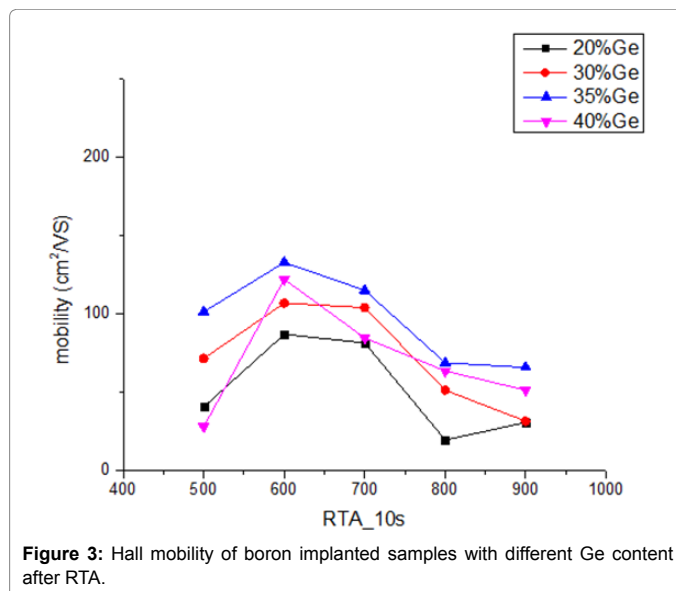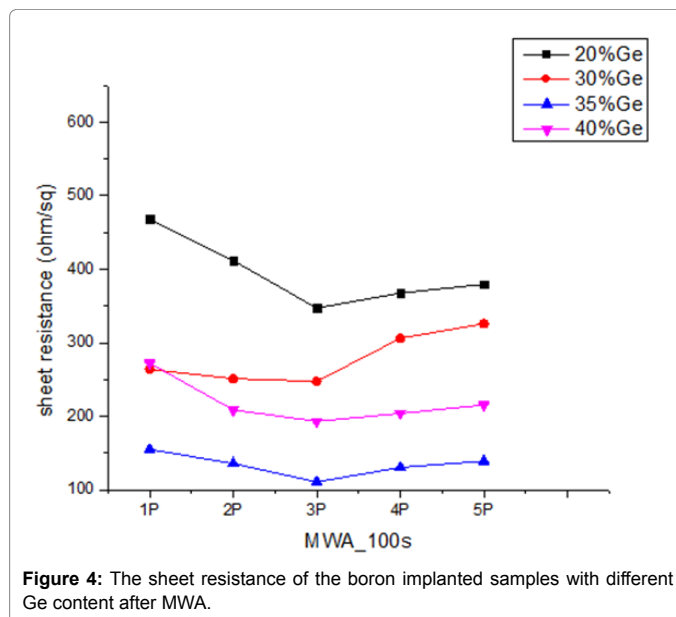

Figure 4: The sheet resistance of the boron implanted samples with different Ge content after MWA.

MWA. Here we investigate whether MWA can also fully activate SiGe: B due to its low thermal temperature and can generate heat directly inside the exposed material in the form of molecular rotational or polarization energies and the energies are transferred throughout the material. Figure 6 shows the x-ray diffraction (XRD) measurement of B implanted into 35% Ge samples annealed by RTA-600°C and MWA-3P. The MWA-3P sample shows a clearer fringe signal than RTA-600°C. The more distinct fringes of the MWA-3P sample signal represent the better quality of the epitaxial layer.

Typically, ion implantation will cause channeling tails. A pre-amorphizing implant can avoid this problem while increasing the

		20%	30%	35%	40%
Sheet resistance (ohm/sq.)	RTA	482	420	169	181
	MWA	348	250	118	208
Mobility (cm²/VS)	RTA	80	109	135	120
	MWA	81	145	172	128

Table 3: Sheet resistance (Rs) and Mobility of different Ge content annealed by RTA at 600°C and MWA at 3P.
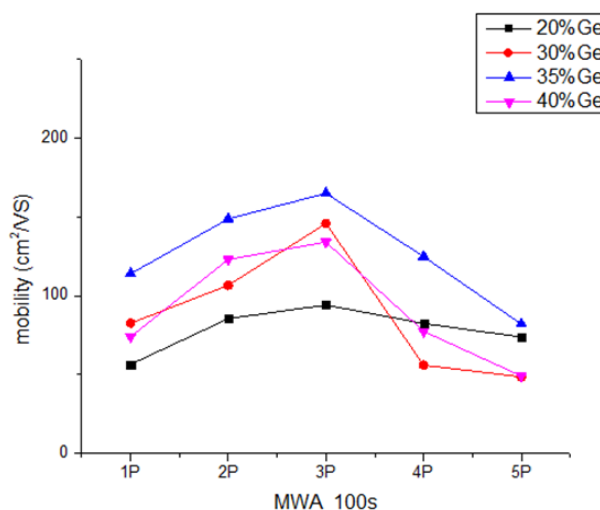

Figure 5: Hall mobility of boron implanted samples with different Ge content after MWA.
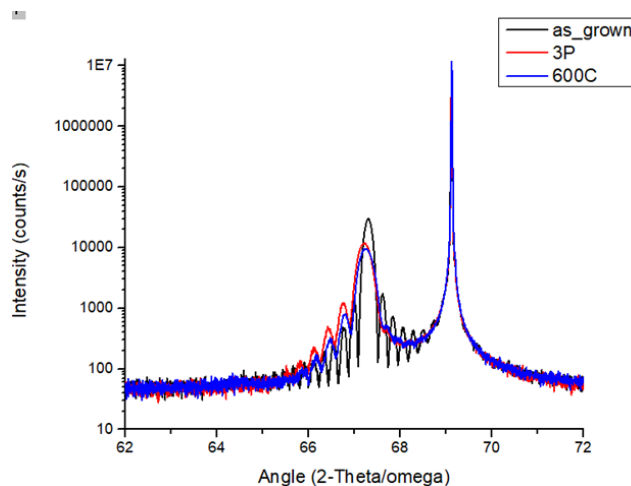

Figure 6: XRD measurement of 35% Ge samples with boron implanted annealing by RTA 600°C and MWA 3P.

activation level and achieving an ultra-shallow junction. Figure 7 shows the SIMS profiles of SiGe implanted with B, Si PAI+B, and Ge PAI+B. Transient-enhanced diffusion is evident at the tail, but there is almost no change in the high doping concentration. By using PAI process, both Si PAI and Ge PAI removed the observable tail TED. However, at the deeper level, Ge PAI can further suppress the channeling tail.

Figure 8 shows the SIMS profiles of SiGe implanted with B, Si PAI+B, and Ge PAI+B samples in the as-implanted state and after an RTA at 600°C. It is observed that without the PAI process, boron has gathered to the end of range damage around 80 nm depth during RTA annealing.

In Si PAI and Ge PAI samples, EOR damage is successfully avoided and boron ions have moved towards the surface. SIMS profiles were also measured for MWA samples. Figure 9 shows the SIMS profiles of SiGe implanted with B, Si PAI+B and Ge PAI+B after MWA at 3P. Both PAI samples exhibit less diffusion than the non-PAI sample, and Ge PAI is slightly better than Si at suppressing tail diffusion. It can also seem in sheet resistance (Figure 10) and hall mobility (Figure 11), Ge PAI and Si PAI samples are both start activation at about 600°C to 700°C, but the sheet resistance of Ge PAI is lower than the Si PAI. Otherwise, hall mobility of Ge PAI is higher than Si PAI. After the regrowth of a PAI
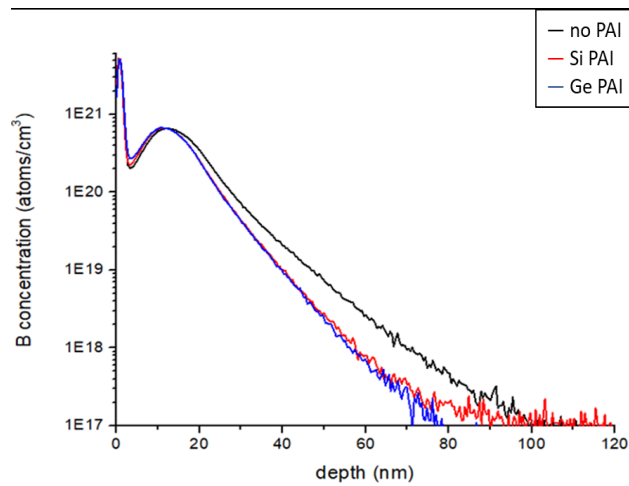
Figure 7: SIMS profiles of implanted B (2 keV at 3 × 10^{15} cm^{-2}, and 1 keV at 2 × 10^{15} cm^{-2}), Ge PAI (10 keV at 1 × 10^{15} cm^{-2})+B and Si PAI (5.5 keV at 1 × 10^{15} cm^{-2})+B.
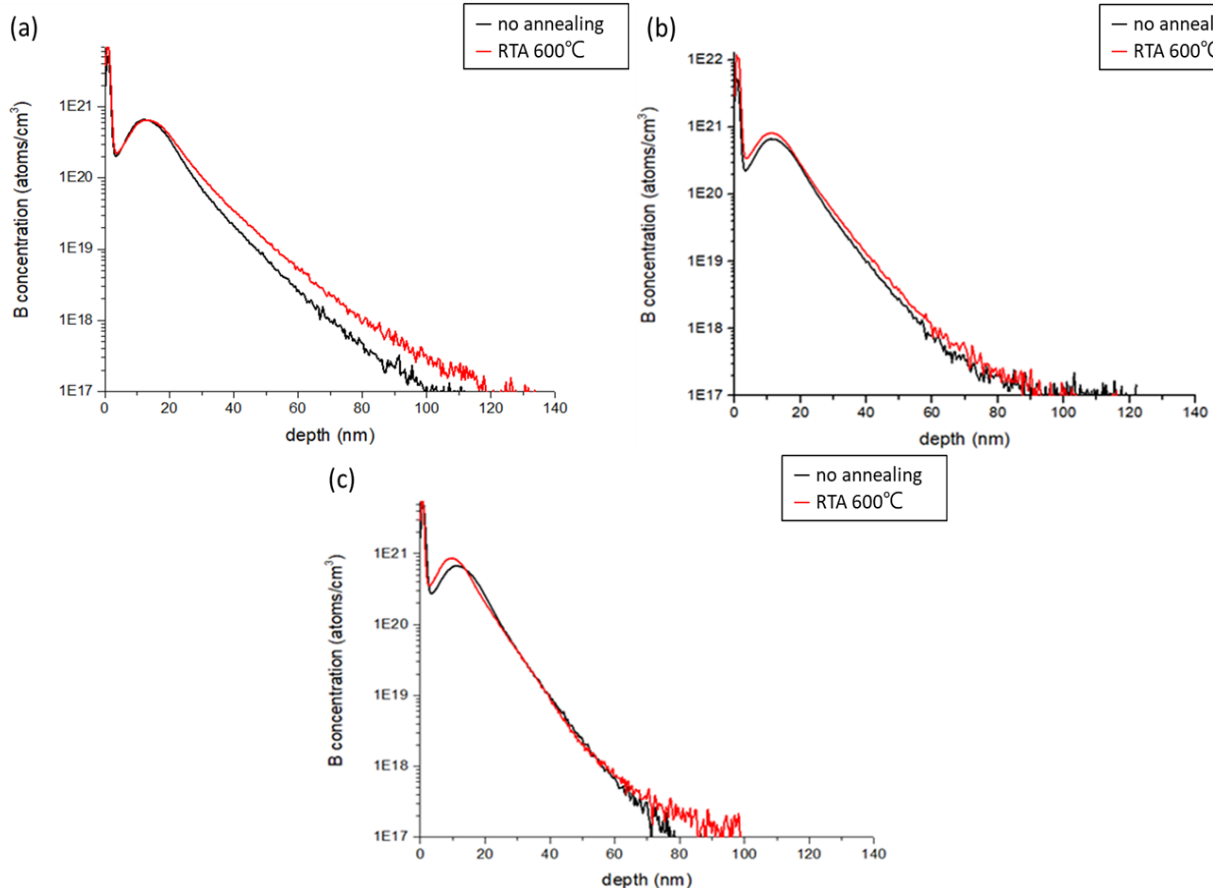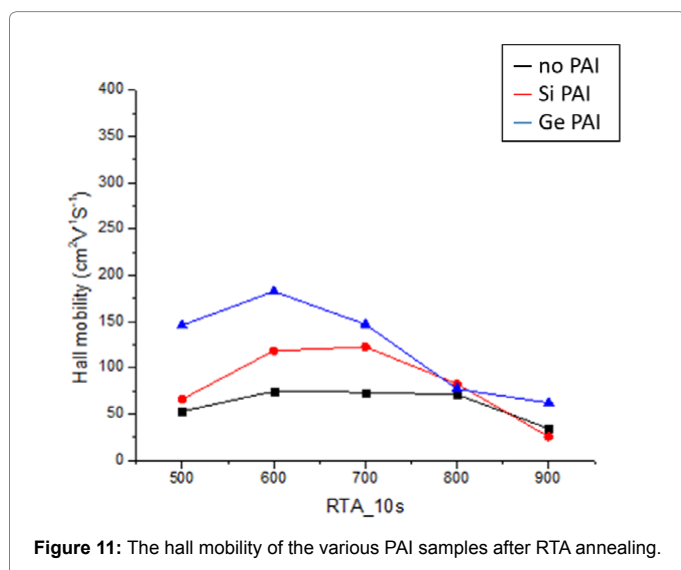

Figure 8: SIMS profiles of (a) implanted B (2 keV at 3 × 10^{15} cm^{-2}, and 1 keV at 2 × 10^{15} cm^{-2}) (b) Si PAI (5.5 keV at 1 × 10^{15} cm^{-2})+B and (c) Ge PAI (10 keV at 1 × 10^{15} cm^{-2})+B w/o RTA-600°C.

SiGe layer, under low B diffusion situation, we can infer that the Ge pre-implant is more helpful for the electrical performance.

Conclusion

This paper investigates the best electrical performance (low sheet resistance and diffusion, high mobility) in SiGe alloys with various Ge contents. The results show that Si capping layer can effectively prevent the surface roughness increase from ion implantation, which in turn reduces its sheet resistance. And with increasing Ge content, the sheet resistance decreases. However, this effect saturates when the Ge content
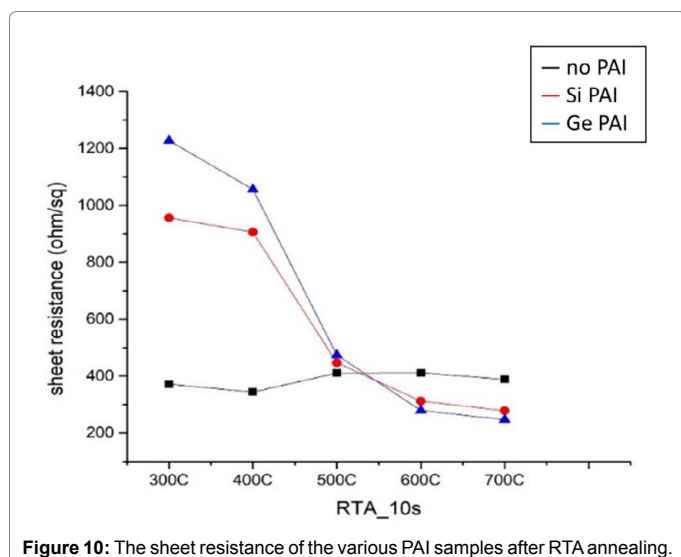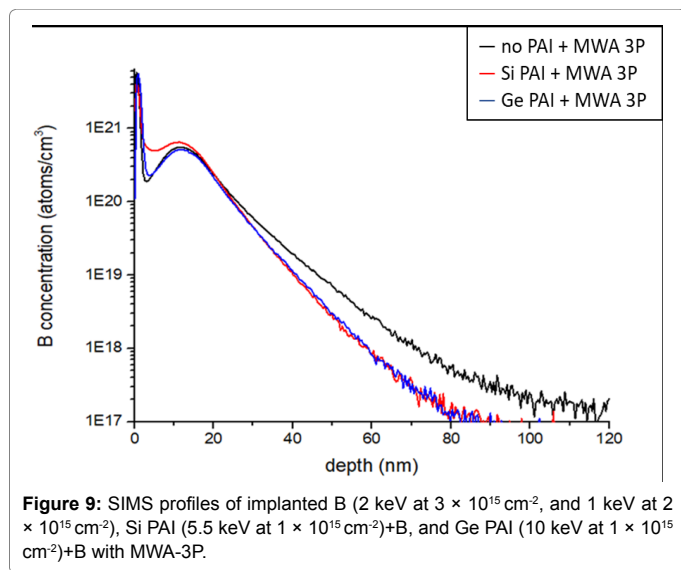
Figure 9: SIMS profiles of implanted B (2 keV at 3×10^{15} cm^{-2}, and 1 keV at 2×10^{15} cm^{-2}), Si PAI (5.5 keV at 1×10^{15} cm^{-2})+B, and Ge PAI (10 keV at 1×10^{15} cm^{-2})+B with MWA-3P.

Figure 10: The sheet resistance of the various PAI samples after RTA annealing.

Figure 11: The hall mobility of the various PAI samples after RTA annealing.

reaches 35% and even degrade when the Ge content becomes 40%.

Si0.65Ge0.35 is an optimum value within situ doped B of 3.2×10^{20} cm^{-2} and two-step (3×10^{15} cm^{-2} and 2×10^{15} cm^{-2}) B implantation. To avoid boron diffusion, Si PAI and Ge PAI are both investigated. Compared to non-PAI, Si or Ge PAI can effectively suppress boron tail diffusion, with Ge PAI showing slightly better results than Si.

Acknowledgments

References

1. Vogler D (2015) The Roadmap to 5nm: Convergence of Many Solutions Needed. SEMICON West.

2. Yamaguchi T, Kawasaki Y, Yamashita T, Yamamoto Y, Goto Y, et al. (2010) Low-resistive and homogenous NiPt-silicide formation using ultra-low temperature annealing with microwave system for 22nm-node CMOS and beyond. International Electron Devices Meeting, IEEE, pp: 26-1.

3. Kowalski JM, Kowalski JE, Lojek B (2007) Microwave annealing for low temperature activation of As in Si. 15th International Conference on Advanced Thermal Processing of Semiconductors, IEEE pp: 51-56.

4. Hu C, Xu P, Fu C, Zhu Z, Gao X, et al. (2012) Characterization of Ni (Si, Ge) films on epitaxial SiGe (100) formed by microwave annealing. Applied Physics Letters 101: 092101.

5. Alford TL, Thompson DC, Mayer JW, Theodore ND (2009) Dopant activation in ion implanted silicon by microwave annealing. Journal of Applied Physics 106: 114902.

6. Fong SC, Wang CY, Chang TH, Chin TS (2009) Crystallization of amorphous Si film by microwave annealing with SiC susceptors. Applied Physics Letters 94: 102104.

7. Pankratov EL (2008) Redistribution of dopant during microwave annealing of a multilayer structure for production p−n junction. Journal of Applied Physics 103: 064320.

8. Thompson K, Booske JH, Gianchandani Y, Cooper R, Bykov Y, et al. (2001) Electromagnetic induction heating for cold wall rapid thermal processing. 9th International Conference on Advanced Thermal Processing of Semiconductors, RTP 2001, IEEE pp: 190-196.

9. Kohli P, Ganguly S, Kirichenko T, Li HJ, Banerjee S, et al. (2002) Microwave annealing for ultra-shallow junction formation. Journal of electronic materials 31: 214-219.

10. Moore GE (1965) Excerpts from a conversation with Gordon Moore: Moore's Law. Video Transcript, Intel, 54.

11. Moore G (2005) Excerpts from a conversation with Gordon Moore: Moore's law. Intel Corporation Document, 1.

12. Shih TL, Su YH, Lee WH (2016) High dopant activation of phosphorus in Ge crystal with high-temperature implantation and two-step microwave annealing. Applied Physics Letters 109: 122103.

13. Taur Y, Ning TH (2013) Fundamentals of modern VLSI devices. Cambridge university press.

14. Dennard RH, Gaensslen FH, Rideout VL, Bassous E, LeBlanc AR (1974) Design of ion-implanted MOSFET's with very small physical dimensions. IEEE Journal of Solid-State Circuits 9: 256-268.

15. Kumar M (2015) Effects of Scaling on MOS Device Performance. IOSR Journal of VLSI and Signal Processing 5: 25-28.

16. Shih TL, Lee WH (2016) High dopant activation and diffusion suppression of phosphorus in Ge crystal with high-temperature implantation by two-step microwave annealing. ECS Transactions 72: 219-225.

17. Lee WH, Tsai MH, Liao WH (2014) Studies on ultra shallow junction 20nm P-MOS with 250°C microwave annealing for activation of boron dopants in silicon. 20th International Conference on Ion Implantation Technology (IIT), IEEE pp: 1-4.